

# Light microscopy of organized monolayers

Dietmar Mobius

The molecular organization strongly influences the optical properties of monolayers. Light microscopic techniques have provided new insights into the relation between molecular packing and the morphology of monolayers, phase transitions, the shape and inner structure of domains as well as the behavior of binary mixtures. Photochemical transformations in organized monolayers have been investigated with these techniques. The phenomena observed with light microscopic techniques have been rationalized by theories providing new access to structural, energetic and mechanical parameters of the ultrathin systems.

## Address

Max-Planck-Institut für biophysikalische Chemie, Postfach 2841, D-37018 Göttingen, Germany; e-mail: dmoebiu@gwdgv1.dnet.gwdg.de

Current Opinion in Colloid & Interface Science 1996, 1:250-256

© Current Science Ltd ISSN 1359-0294

## Abbreviations

<b>BAM</b>	Brewster angle microscopy
<b>BOO</b>	long range bond orientational order
<b>PFM</b>	polarized fluorescence microscopy
<b>SNOM</b>	scanning near field optical microscopy
<b>SPM</b>	surface plasmon microscopy
<b>TOO</b>	long range tilt orientational order

## Introduction

Insoluble monolayers are generally formed at the air/water interface by spreading a solution of an amphiphile on the surface of a trough [1]. After evaporation of the solvent, the lipid molecules may be compressed by reducing the macroscopic area with a movable barrier. The surface pressure versus area isotherm obtained in this way provides evidence for phase transitions in such two-dimensional systems, and a large variety of phases has been found [2]. Phase transitions in lipid monolayers have been observed directly by fluorescence microscopy [3]. In this technique, a fluorescent probe molecule is added to the lipid. The contrast between coexisting phases results from the distribution and/or different fluorescence quantum yield of the probe in the different phases. The spatial distribution of the fluorescence lifetime due to the different environment of the emitting chromophore is recorded in fluorescence lifetime imaging microscopy [4]. Cell surfaces have been studied, but according to my knowledge, monolayers have not been investigated by this method so far.

The presence of a probe molecule is not required in Brewster angle microscopy (BAM) [5,6]. This technique is based on the fact that p-polarized light is not reflected at an interface when incident under the Brewster angle, which is about 53° for the air/water interface when using

visible light. If the angle is kept constant, formation of a monolayer changes the optical situation, and the observed reflectivity of the system depends on the optical properties of the ultrathin film. Monolayers and monolayer systems on transparent solids may also be characterized by BAM [7]. A monolayer, according to its optical properties, on a metal surface modifies the excitation of surface plasmons by changing the resonance condition, that is, the angle of incidence under which the reflectivity of the system vanishes. This is the basis of surface plasmon microscopy (SPM) [8], which provides important information on laterally structured thin films on metals and complements BAM that is restricted to thin films on transparent solids.

Although the information in these methods is carried by light in the far field of the emitter, so limiting the lateral resolution, scanning near field optical microscopy (SNOM) allows one to observe objects with a spatial resolution of 30 to 50 nm [9]. Scanning techniques other than the optical methods for example, scanning force microscopy [10] or scanning tunneling microscopy which provide information with high resolution, will not be discussed here.

## Monolayer phases and phase transitions

Insoluble monolayers undergo several phase transitions upon compression. The liquid phase shows no textures (i.e. no particular pattern of brightness variations across the image), due to the high mobility of the amphiphile molecules and disordered hydrocarbon chains. A large variety of ordered phases is observed at higher surface pressures.

### Liquid phase of binary mixtures

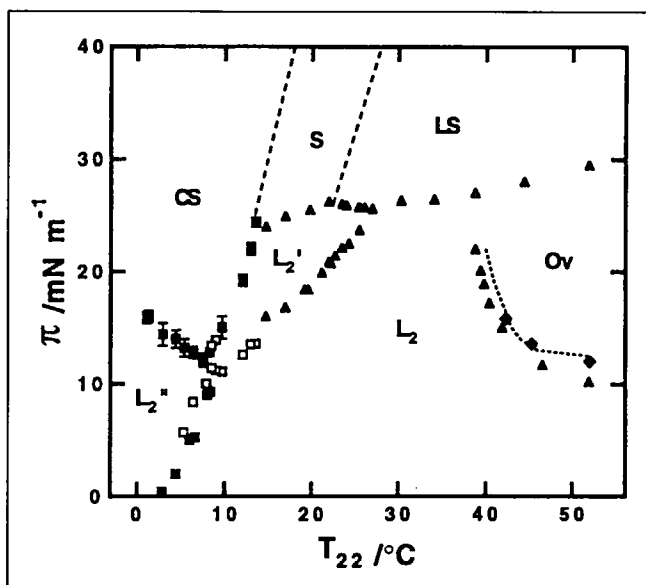
In monolayers of binary mixtures of phospholipids and steroids at the air/water interface, coexisting two-dimensional liquid phases have been observed by fluorescence microscopy [11]. McConnell, who has contributed considerably to the understanding of domain shapes, and his group have recently investigated electric field induced concentration gradients in such mixed monolayers [12]. Inhomogeneous electric fields have been used to manipulate domains of ordered phase [13]. An inhomogeneous electric field induces phase separation and formation of domains in a liquid phase binary monolayer of dihydrocholesterol and dimyristoyl-phosphatidylcholine that is in the homogeneous region of the phase diagram below the critical surface pressure [14••]. Above the critical pressure, concentration gradients are formed by the inhomogeneous electric field [14••]. Such mixed monolayers, at certain temperatures and surface pressures, may separate into phospholipid-rich and cholesterol-rich phases, and gas domains form at the interface between these two phases upon expansion to low surface pressures. Coexistence of these three phases has been observed by

fluorescence microscopy [15<sup>o</sup>], and the analysis of the domain shapes yields relative line tensions of the domain boundaries.

#### Long range order

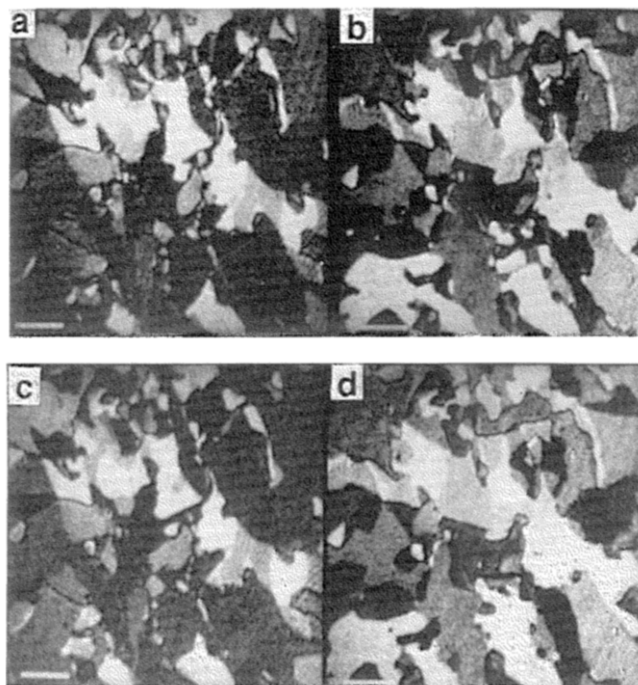
A part of the phase diagram of docosanoic acid (22 C atoms) monolayers [16<sup>o</sup>] is shown in Figure 1. The molecular packing in these condensed phases has been determined by X-ray scattering and reflection studies requiring high intensity synchrotron radiation. In an analogy to smectic liquid crystals, several phases are characterized by long range tilt orientational order (TOO). Taking into account that the polarizability of an extended hydrocarbon chain is larger along the axis than perpendicular to the axis, optical anisotropy of domains with TOO is expected and observed by BAM if the domains are at least several microns in diameter. Domains with different azimuthal orientations have a different brightness, as shown in Figure 2 for a monolayer of docosanoic acid on water at 14°C at the  $L_2 \rightarrow L_2'$  transition [16<sup>o</sup>] (the phases are indicated in Figure 1). Such domains can also be recorded by polarized fluorescence microscopy (PFM), however, with much less contrast [16<sup>o</sup>]. Figure 2 shows the same area through multiple compression/relaxation cycles. Obviously, the initial texture is recovered if the monolayer of docosanoic acid is kept for a few minutes only in each phase. Similar reversible effects have been observed in monolayers of other fatty acids [17].

Figure 1



Generalized phase diagram of n-alkanoic acids. The part of the phase diagram consisting of only condensed phases is shown in this plot of surface pressure  $\pi$  versus temperature  $T_{22}$  for the case of docosanoic acid (22 C atoms). The phase transitions have been determined by different techniques as indicated by different symbols (for details, see [16<sup>o</sup>]). The phases denoted  $L_2$ ,  $L_2'$ ,  $L_2''$ , and  $Ov$  are phases with tilted hydrocarbon chains. In phases  $LS$ ,  $S$ , and  $CS$  the chains are oriented normal to the monolayer plane. Reproduced with permission from [16<sup>o</sup>].

Figure 2



Memory effect of monolayer texture. BAM images of the  $L_2 \rightarrow L_2'$  transition in monolayers of docosanoic acid at 14°C. The texture is unchanged through repeated compression/expansion cycles.  $L_2$  phase: a and c;  $L_2'$  phase: b and d. The bars represent 50  $\mu\text{m}$ . Reproduced with permission from [16<sup>o</sup>].

The phase transition between the two phases  $L_2$  and  $Ov$ , that differ only in the tilt direction (to next neighbor and next nearest neighbor, respectively), is not visible in the surface pressure versus area isotherm and has been discovered by BAM [17], and confirmed by PFM [18]. The boundary between  $L_2$  and  $Ov$  as determined by PFM is about  $1 \text{ mN m}^{-1}$  lower than that determined by BAM due to the presence of the fluorescent probe [16<sup>o</sup>]. Another, more important, difference between the two techniques is the higher contrast in BAM. Therefore, the weak optical anisotropy of a phase with long range bond orientational order (BOO) of hydrocarbon chains that are oriented normal to the monolayer plane, such as the  $S$  phase (orthorhombic packing of the hydrocarbon chains), causes a detectable contrast between domains of different azimuth in BAM [19<sup>o</sup>]. Based on computer simulations, a simple and elegant procedure has been developed to determine the reason, either TOO or BOO, for optical anisotropy in the plane [19<sup>o</sup>]. When rotating the sample in the Brewster angle microscope horizontally by  $360^\circ$ , thus changing the azimuth angle, the brightness of a selected domain shows maxima and minima. The optical anisotropy is caused by TOO if one maximum and one minimum occurs for a particular analyzer angle, whereas two maxima and two minima are observed for BOO.

### Evaluation of structural parameters

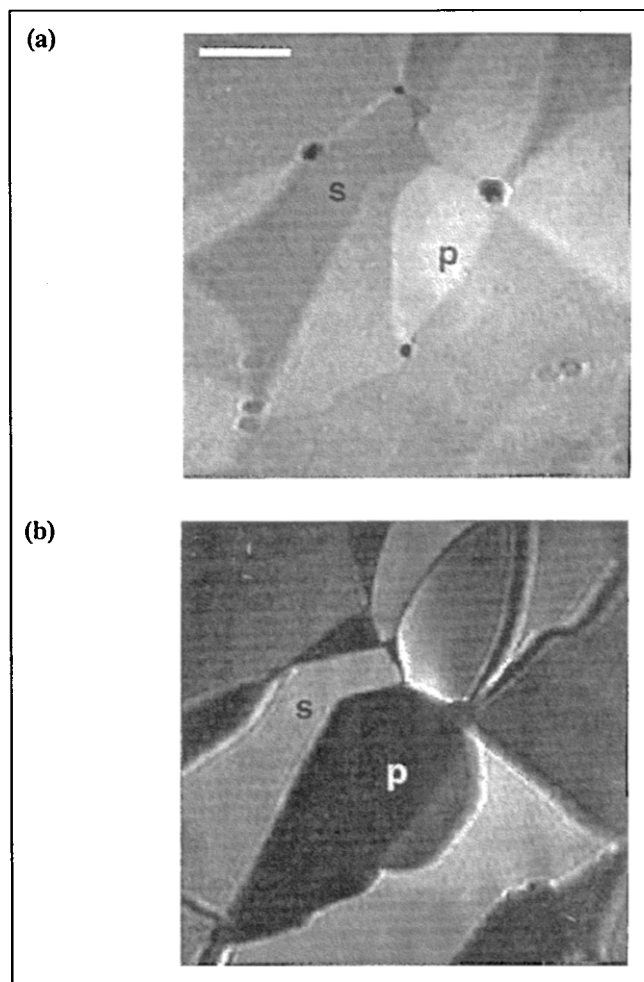
The current attempts [19\*,20\*,21,22] to obtain a quantitative description of reflectivity of the air/monolayer/substrate system with light incident under the Brewster angle of the air/substrate interface are based on Berreman's  $4 \times 4$  matrix formalism [23]. In general, adequate values for the unknown parameters (refractive indices, thickness, tilt angle) have to be put into the equations to calculate the reflectivity of a domain with TOO. The particular condition of Brewster angle, however, permits some simplification, and from a set of three reflectivities measured under selected conditions (analyzer angle), the tilt angle and two refractive indices have been evaluated in a particular case by Hönig [24\*\*]. The procedure shown in Figure 3 is taken from [24\*\*], where the reflected intensities of a domain oriented parallel to the plane of the incident light with the analyzer in the p direction ( $I_{pp}$ ), a domain oriented in the s direction with the analyzer in p direction ( $I_{sp}$ ), and a domain oriented in the s direction with analyzer in the s direction ( $I_{ss}$ ) are measured. From these intensities, the refractive indices along a hydrocarbon chain,  $n_3 = 1.53 \pm 0.01$ , and normal to the chain axis,  $n_1 = 1.47 \pm 0.01$ , as well as the tilt angle  $\theta = 35^\circ \pm 3^\circ$  have been evaluated for a monolayer of eicosanoic acid. The angle is in excellent agreement with that determined by X-ray studies [25]. This example shows that important structural information including quantitative parameters is now accessible from fast and simple optical measurements, as compared to X-ray studies which require long term data acquisition with synchrotron radiation.

### Miscibility and phase separation

Monolayers of two or more components have been formed frequently by spreading mixed solutions [1]. In particular, amphiphilic dyes have been incorporated in monolayers of long chain fatty acids acting as a matrix. Therefore, investigations of binary and tertiary systems are particularly needed. The phase diagram of monolayers of fatty acid-alcohol mixtures has been investigated by PFM and BAM by Knobler and co-workers [26\*], as well as by X-ray diffraction by Dutta's group [27]. As in the case of pure fatty acid monolayers (docosanoic acid, see Figure 1), the mixed heneicosanoic acid-heneicosanol monolayers show the  $L_2$ ,  $L_2'$ , and Ov phases and the  $L_2 \rightarrow L_2'$  and  $L_2 \rightarrow Ov$  transitions, depending on the molar fraction of the alcohol. The phase boundaries move with composition, and at a fraction of 0.23 alcohol, the  $L_2 \rightarrow L_2'$  and  $L_2 \rightarrow Ov$  transitions merge.

Miscibility of myristic acid and 7-(2-anthryl)heptanoic acid has been studied by BAM [28]. These quite different components form mixed monolayers at large molar fractions of myristic acid, in particular in the liquid phase. At higher surface pressure, phase separation is observed. In fact, such behavior is the basis of fluorescence microscopy, which requires a different distribution of the probe between different phases of the host monolayer. Phase separation in a mixed monolayer of cholesterol and

Figure 3



Evaluation of optical and structural parameters. BAM images of a monolayer of eicosanoic acid on water. Determination of the reflected intensities (a)  $I_{pp}$  of a domain with molecules tilted in the direction of the incident p-polarized light, analyzer in p polarization, and reflected intensities  $I_{sp}$  of a domain with tilt in the s direction, analyzer in p polarization; (b) measurement of  $I_{ss}$  of the domain with tilt in s direction, analyzer in s polarization. From these intensities, the tilt angle and the refractive indices along the hydrocarbon chain ( $n_3$ ) and perpendicular to the chain are calculated. Reproduced with permission from [24\*\*].

an amphiphilic azobenzene derivative is discussed in the section 'Photoprocesses' below.

### Defects

Monolayers show the same type of defect structures as smectic liquid crystals, such as shell (droplet), star, and stripe defects upon a phase transition to a phase with tilted hydrocarbon chains. Recent simulations, based on bend or splay of the azimuthal orientation, using realistic parameters have revealed the inner structure of such defects. An example is given in Figure 4a for a shell texture in the LC- $L_1$  coexistence region of a monolayer of pentadecanoic acid recorded by BAM [20\*]. Figure 4b shows the brightness distribution according

to the simulation, with the particular type of splay of azimuthal orientations of the hydrocarbon chains in the shell presented schematically in Figure 4c. The in-plane molecular orientations follow straight lines crossing at a defect point just inside or rejected outside the shell. The chains are pointing with their end groups to the defect point. Other orientations, including those where the chains are pointing away from this point, result in totally different brightness distributions. Therefore, the inner structure of this defect can be determined unambiguously by comparison with simulations. A detailed analysis by Rivière and Meunier [29\*\*] of the position of the virtual defect point outside of two-dimensional drops and of the elongation of the drop as a function of the drop size provides an insight into the anisotropic line tension of the drop and the elastic constants. In large drops (diameter 300  $\mu\text{m}$ ) the defect point is close to the drop boundary, whereas in small drops (60  $\mu\text{m}$ ), which are more elongated than the large drops, this point may be far away from the border (110 to 120  $\mu\text{m}$  in distance). The azimuth of the orientation of the chains at the drop boundary is no longer normal to the boundary. Ratios of the anisotropic line tension and the elastic constant were determined with a model used for the calculation of elastic constants in similar defect structures in liquid crystals (smectic I phase) [30]. Surprisingly, the splaying energy is larger than the bending energy, although the texture presents more splay than bend [29\*\*].

Another defect structure consisting of splay of the hydrocarbon chains is the star defect that very often shows six segments of different brightness [20\*]. Recently, an interesting observation was made by Vollhardt and co-workers [31]. They observed the transformation of a star defect with seven segments to a defect with six segments upon compression of a monolayer of 1-monopalmitoyl-*rac*-glycerol. An example of this defect is shown in Figure 5 [32\*\*]. For this system, detailed X-ray diffraction measurements have been done which provide information on the change of the lattice upon compression [32\*\*]. The chain projections form a rectangular lattice with tilt azimuth parallel to the  $a$  axis (10). Low index

directions like (31) and (31) should possess low defect line energies and therefore should promote a jump of the molecular orientation. The angle between these directions at a surface pressure of 5.5  $\text{mN m}^{-1}$  is 53.4° and increases to 57.9° at 44  $\text{mN m}^{-1}$ . The observed angle between the segment boundaries in the seven-fold star defect is  $\delta = 50\text{--}55^\circ$  (as compared to  $360/7 = 51.5$ ). The model of defect lines following low index lattice directions explains nicely the observed transition [32\*\*].

Recent theoretical treatments of domain shapes and patterns [33], the hydrodynamics of quantized shape transitions [34] as well as instabilities of stripe textures [35] rationalize light microscopic observations of monolayers.

### Monolayer transfer to solid substrates

Monolayers may be transferred from the air/water interface to solid substrates by dipping the solid through the monolayer, while keeping the surface pressure constant via a feedback system. It is generally assumed that the change of the head group environment causes a modification of molecular packing during transfer. Domain melting has been observed [36\*] when monolayers of phospholipids doped with fluorescent probes have been transferred to silicon wafers having a natural oxide layer. This domain melting is due to the different mixing behaviors of probe and host near the three-phase line causing local compositional differences. The results were interpreted in the frame of a two-dimensional analogy of three-dimensional solidification [36\*]. Concentration gradients of the probe at the LC/LE domain boundary of phospholipid monolayers transferred to a glass substrate have been observed by SNOM [9\*]. This type of phospholipid monolayer, however, is rarely used in the construction of organized monolayer assemblies. Furthermore, it is necessary to eliminate the fluorescent probe. In preliminary experiments with BAM, no change in the domain structure and texture has been seen upon transfer of a monolayer of heneicosanoic acid to glass substrates (DB Spohn, D Hönig, D Möbius, unpublished data).

**Figure 4**

Determination of the molecular organization in a shell defect. (a) BAM image of a shell defect with light incident from the lower side; (b) simulated brightness distribution using reasonable optical parameters. The particular pattern of tilt orientation of the hydrocarbon chains in the defect is shown in (c). The molecules are anchored at the water surface and the chain ends are pointing to the interior of the defect. Other arrangements, for example, with the chain ends pointing outward, result in quite different brightness distributions. Reproduced with permission from [20\*].

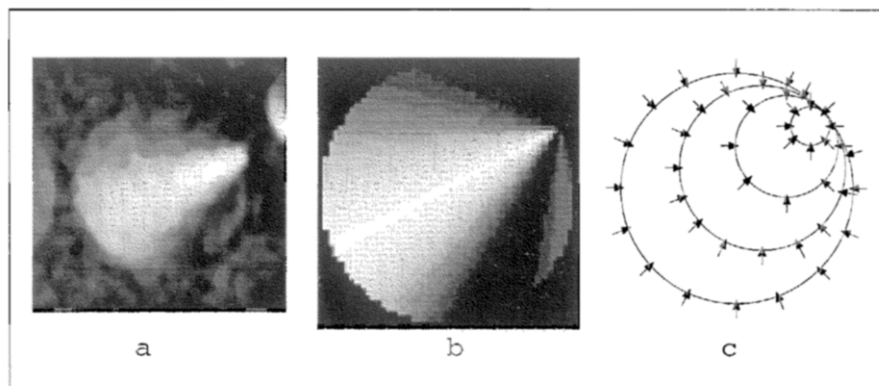
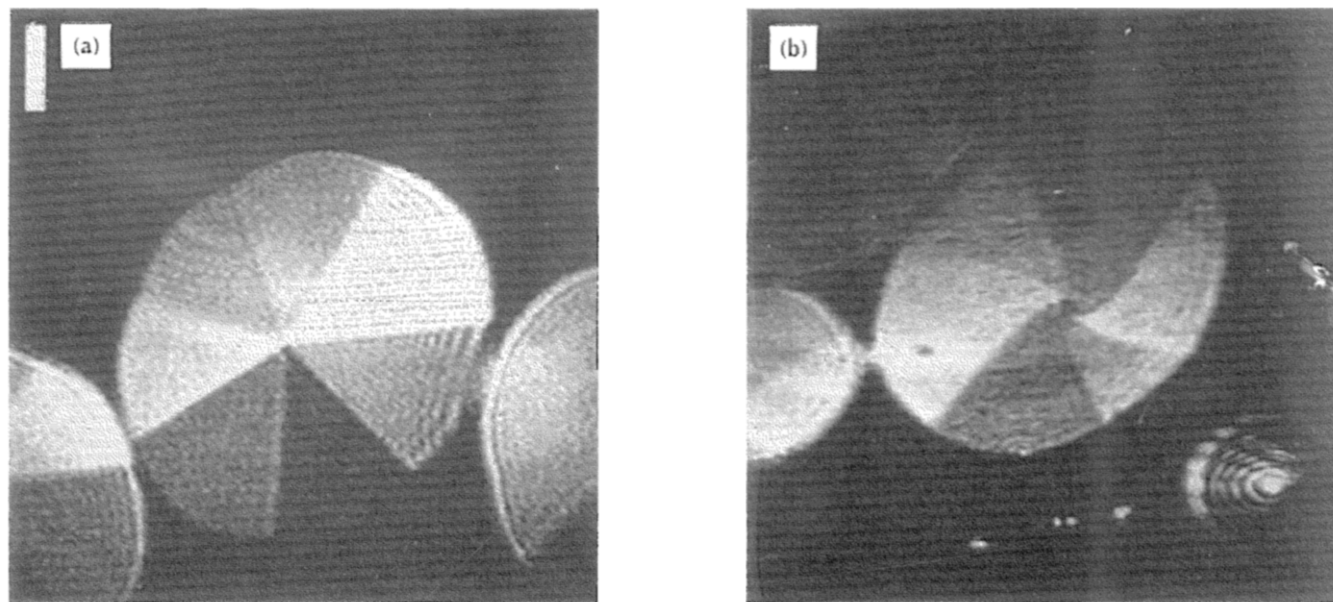


Figure 5



Star defect changing the number of segments upon compression. BAM images of condensed phase domains in a monolayer of 1-monopalmitoyl-*rac*-glycerol. **(a)** At compression in the plateau region of the surface pressure versus area isotherm ( $\sim 5.5 \text{ mN m}^{-1}$ ), star defects with seven segments corresponding to different azimuths of molecular tilt are observed. **(b)** When the monolayer is kept for about 30 min at high surface pressure (about  $45 \text{ mN m}^{-1}$ ) defects with six segments are observed. This phenomenon has been related to the change of the lattice structure upon compression. The bar represents  $100 \mu\text{m}$ . Reproduced with permission from [32\*\*].

The deposition effects of monolayers of docosanoic acid in a wide range of surface pressures have been investigated by determining the tilt angle using reflection high energy electron diffraction [37\*]. The tilt angle is a parameter much more sensitive to lateral pressure than the unit cell parameters. This angle differs on the solid substrate from that on the water surface just before deposition. This behavior has been rationalized by the principle of equivalent states.

### Photoprocesses

Phototransformation of a molecule very often causes a change in its optical properties, and attempts are currently being made to use ultrathin films with such photoactive molecules for information storage. Even far away from the optical absorption band, that is non-resonant, such modifications can be observed by microscopic techniques sensitive to refractive index changes, such as BAM and surface plasmon microscopy (SPM). Many materials undergoing reversible photoisomerization are based on the azobenzene chromophore. For example, multilayer systems of a polymer with side-chain azobenzene on thin metal films (i.e. Cr, 4 nm thick and Au, 50 nm thick) have been investigated by SPM and reflectivity measurements [38]. After illuminating the sample with UV radiation through a mask, the photoisomerization pattern is clearly visible in the SPM image.

Amphiphilic azobenzene derivatives have also been used for the study of reversible photoisomerization in or-

ganized monolayers. In mixed monolayers of the dye with cholesterol (molar ratio of dye:cholesterol, 1:4) at the air/water interface, phase separation is observed by BAM [39\*]. With the cholesterol phase as internal standard the photoreaction is directly visible by a contrast reversal because the domains of *cis* isomer reflect more than the cholesterol phase, whereas the *trans* isomer domains appear darker than the cholesterol [39\*]. A specifically designed mixed monolayer was prepared to achieve unconstrained isomerization despite the different molecular areas of the *cis* and *trans* isomers [40]. As in surface plasmon microscopy, BAM can be done in a non-resonant way, thereby avoiding any photochemical change of the system as a result of the inspection.

Photoreorientation of azobenzene chromophores in monolayers has been studied in thin films on glass, both by polarized reflection microscopy and by scanning force microscopy. Polarized irradiation leading to in-plane reorientation of the molecules does not drastically influence the structure, as shown by only small differences between illuminated and non-illuminated areas of film [41]. Two-dimensional dynamic patterns have been generated in monolayers of an amphiphilic azobenzene derivative at the air/water interface and observed by polarized reflection microscopy [42\*\*]. A phase with a stripe texture of tilted chromophores (smectic C) is formed. Upon illumination with polarized light a reorientation of the molecules due to photoisomerization causes a change of the static pattern followed by spontaneous generation of two-dimensional traveling orientational waves in the monolayer.

## Conclusion

Optical microscopic techniques are particularly suited for the characterization of condensed monolayer phases. Important achievements during the period from mid-1994 to the end of 1995 comprise the optical identification of different types of long range order, and the evaluation of detailed structural information from the observed textures. The analysis of domain shapes has provided access to parameters such as elasticity and line tension at the boundary between two phases. Phototransformations in monolayers and multilayer systems were investigated by non-resonant optical techniques. SNOM provided information on structural features and probe distribution at the border between two phases with a 50 nm lateral resolution. The combined results obtained recently by optical methods have strongly enhanced our understanding of molecular organization and intermolecular interactions.

## References and recommended reading

Papers of particular interest, published within the annual period of review, have been highlighted as:

- of special interest
  - of outstanding interest
1. Kuhn H, Möbius D: **Monolayer assemblies.** In *Investigations of Surfaces and Interfaces*. Edited by Rossiter BW, Baetzold RC. New York: John Wiley & Sons Inc; 1993:375–542.
  2. Bibo AM, Knobler CM, Peterson IR: **A monolayer phase miscibility comparison of long-chain fatty acids and their ethyl esters.** *J Phys Chem* 1991, **95**:5591–5599.
  3. Lösche M, Sackmann E, Möhwald H: **A fluorescence microscopic study concerning the phase diagram of phospholipids.** *Ber Bunsenges Phys Chem* 1983, **87**:848–852.
  4. Gadella TWJ, Jovin TM, Clegg RM: **Fluorescence lifetime imaging microscopy (FLIM): spatial resolution of microstructures on the nanosecond time scale.** *Biophys Chem* 1994, **48**:221–239.
  5. Hénon S, Meunier J: **Microscope at the Brewster angle. Direct observation of first-order phase transitions in monolayers.** *Rev Sci Instr* 1991, **62**:936–939.
  6. Höning D, Möbius D: **Direct visualisation of monolayers at the air-water interface by Brewster angle microscopy.** *J Phys Chem* 1991, **95**:4590–4592.
  7. Höning D, Möbius D: **Brewster angle microscopy of LB films on solid substrates.** *Chem Phys Lett* 1992, **195**:50–52.
  8. Aust EF, Sawodny M, Ito S, Knoll W: **Surface plasmon and guided optical wave microscopies.** *Scanning* 1994, **16**:353–361.
  9. Hwang J, Tamm LK, Böhm C, Ramalingam T, Betzig E, Edidin M: **Nanoscale complexity of phospholipid monolayers investigated by near-field scanning optical microscopy.** *Science* 1995, **270**:610–614.
- This paper presents important data on the morphology of monolayers and fluorescence probe concentration gradients at phase boundaries with a lateral resolution of 50 nm.
10. Chi LF, Fuchs H, Johnston RR, Ringsdorf H: **Investigations of phase-separated Langmuir-Blodgett-films by atomic force microscopy.** *Thin Solid Films* 1994, **242**:151–156.
  11. McConnell HM: **Structures and transitions in lipid monolayers at the air-water interface.** *Annu Rev Phys Chem* 1991, **42**:171–195.
  12. Lee KYC, Klingler JF, McConnell HM: **Electric field-induced concentration gradients in lipid monolayers.** *Science* 1994, **263**:655–658.
  13. Miller A, Möhwald H: **Collecting two-dimensional phospholipid crystals in inhomogeneous electric fields.** *Europhys Lett* 1986, **2**:67–74.
  14. Lee KYC, McConnell HM: **Effect of electric-field gradients on lipid monolayer membranes.** *Biophys J* 1995, **68**:1740–1751. Clear and comprehensive description of the effect of inhomogeneous electric fields on binary monolayers in the liquid phase, visualized by fluorescence microscopy and including model calculations that are interesting in connection with biological membranes.
  15. Hagen JP, McConnell HM: **Three-phase intersection points in monolayers.** *Colloid Surface A* 1995, **102**:167–172. Monolayers of particular binary mixtures show two coexisting phases in the liquid state. Upon decompression, gas domains form, and from the analysis of the domain shapes, relative line tensions are evaluated.
  16. Rivière S, Hénon S, Meunier J, Schwartz DK, Tsao M-W, Knobler CM: **Textures and phase transitions in Langmuir monolayers of fatty acids. A comparative Brewster angle microscope and fluorescence microscope study.** *J Chem Phys* 1994, **101**:10045–10051. This paper provides a clear evaluation of the relative strengths of polarized fluorescence microscopy and Brewster angle microscopy. The different transitions between condensed phases have been investigated by these techniques in a combined effort of two leading groups in this field, and are very clearly discussed.
  17. Overbeck GA, Möbius D: **A new phase in the generalized phase diagram of monolayer films of long chain fatty acids.** *J Phys Chem* 1993, **97**:7999–8004.
  18. Schwartz DK, Knobler CM: **Direct observation of transitions between condensed Langmuir monolayer phases by polarized fluorescence microscopy.** *J Phys Chem* 1993, **97**:8849–8851.
  19. Overbeck GA, Höning D, Wolthaus L, Gnade M, Möbius D: **Observation of bond orientational order in floating and transferred monolayers with Brewster angle microscopy.** *Thin Solid Films* 1994, **242**:26–32. This paper describes a new, simple and elegant method to discriminate between different types of long range order in monolayer mesophases based on Brewster angle microscopy.
  20. Overbeck G, Höning D, Möbius D: **Stars, stripes and shells in monolayers: simulation of the molecular arrangement in Schlieren structures.** *Thin Solid Films* 1994, **242**:213–219. Comparison of Brewster angle images and computer simulations of defect structures in monolayers provides unambiguous information on the inner structure (i.e. the gradual or abrupt change of molecular tilt orientation) of such defects.
  21. Tabe Y, Yokoyama H: **Fresnel formula for optically anisotropic Langmuir monolayers: an application to Brewster angle microscopy.** *Langmuir* 1995, **11**:699–704.
  22. Tsao M-W, Fischer T, Knobler CM: **Quantitative analysis of Brewster-angle microscope images of tilt order in Langmuir monolayer domains.** *Langmuir* 1995, **11**:3184–3188.
  23. Berreman DW: **Optics in stratified and anisotropic media: 4x4-matrix formulation.** *J Opt Soc Am A-Opt Image Sci* 1972, **62**:502–510.
  24. Höning D: **Molekular Organisierte Filme: Laterale Struktur und Optische Eigenschaften [PhD Thesis].** Göttingen: Georg-August-Universität; 1994. [Title translation: Molecularly organized films: lateral structure and optical characteristics.] This PhD thesis marks a considerable progression in the evaluation of structural and optical parameters in tilted monolayer phases from Brewster angle images.
  25. Tippmann-Krayer P, Möhwald H: **Precise determination of tilt angles by X-ray diffraction and reflection with arachidic acid.** *Langmuir* 1991, **7**:2303–2306.
  26. Fischer B, Teer E, Knobler CM: **Optical measurements of the phase diagram of Langmuir monolayers of fatty acid-alcohol mixtures.** *J Chem Phys* 1995, **103**:2365–2368. This paper describes the behavior of condensed phases of binary monolayers investigated with Brewster angle microscopy, including the particularly interesting phenomenon of merging of two tilted phases.
  27. Durbin MK, Shih MC, Malik A, Zschack P, Dutta P: **Isotherm and X-ray diffraction studies of mixed monolayers.** *Colloid Surface A* 1995, **102**:173–179.
  28. Angelova A, Van der Auweraer M, Ionov R, Vollhardt D, De Schryver FC: **Miscibility of alkanolic and  $\omega$ -anthrylalkanoic acids in monolayers at the air/water interface studied by means of Brewster angle microscopy.** *Langmuir* 1995, **11**:3167–3176.
  29. Rivière S, Meunier J: **Anisotropy of the line tension and bulk elasticity in two-dimensional drops of a mesophase.** *Phys Rev Lett* 1995, **74**:2495–2498.

In this excellent paper the inner structure of shell defects (drops, boojums) as characterized by the position of the defect point and distortions of the shell are analyzed. The Brewster angle microscopy observations provide new quantitative data on elasticity constants and anisotropic line tensions.

30. Langer SA, Sethna JP: **Textures in a chiral smectic liquid-crystal film.** *Phys Rev A* 1986, **34**:5035–5046.
  31. Gehlert U, Weidemann G, Vollhardt D: **Morphological features in 1-monoglyceride monolayers.** *J Colloid Interface Sci* 1995, **174**:392–399.
  32. Brezesinski G, Scalas E, Struth B, Möhwald H, Bringezu F, Gehlert U, Weidemann G, Vollhardt D: **Relating lattice and domain structures of monoglyceride monolayers.** *J Phys Chem* 1995, **99**:8759–8762.
- The surprising transition from star defects with seven segments to such defects with six segments in monolayers observed with Brewster angle microscopy depends on the surface pressure. In this paper, the phenomenon is related to changes of the lattice structure upon compression as determined by synchrotron X-ray diffraction.
33. Seul M, Andelman D: **Domain shapes and patterns: the phenomenology of modulated phases.** *Science* 1995, **267**:476–483.
  34. Stone HA, McConnell HM: **Hydrodynamics of quantized shape transitions of lipid domains.** *Proc Roy Soc London A Ser* 1995, **448**:97–111.
  35. De Koker R, Jiang WN, McConnell HM: **Instabilities of the stripe phase in lipid monolayers.** *J Phys Chem* 1995, **99**:6251–6257.
  36. Spratte K, Riegler H: **Steady state morphology and composition of mixed monomolecular films (Langmuir monolayers) at the air/water interface in the vicinity of the three-phase line: model calculations and experiments.** *Langmuir* 1994, **10**:3161–3173.

This paper rationalizes the phenomena observed by fluorescence microscopy at the three-phase line during monolayer transfer from the wa-

ter surface onto a solid. A model in analogy to the three-dimensional thermotropic solidification process in binary alloys is used.

37. Brzezinski V, Peterson IR: **Deposition effects on the structure of Langmuir-Blodgett monolayers of docosanoic acid.** *J Phys Chem* 1995, **99**:12545–12552.

This paper presents a RHEED (reflection high energy diffraction) study of the structure of the first monolayer transferred from the water surface to silicon wafers, and provides an excellent basis for the optical studies of monolayer transfer.

38. Knobloch H, Orendi H, Büchel M, Sawodny M, Schmidt A, Knoll W: **Optical switching of azobenzene sidechain molecules observed by plasmon spectroscopy.** *Fresenius J Anal Chem* 1994, **349**:107–111.
39. Maack J, Ahuja RC, Tachibana H: **Resonant and nonresonant investigations of amphiphilic azobenzene derivatives in solution and in monolayers at the air/water interface.** *J Phys Chem* 1995, **99**:9210–9220.

This paper on the reversible photoisomerization of monolayers of amphiphilic azobenzene derivatives demonstrates the potential of non-resonant Brewster angle microscopy and reflectometry for studying such processes.

40. Ahuja RC, Maack J, Tachibana H: **Unconstrained cis-trans isomerization of azobenzene moieties in designed mixed monolayers at the air/water interface.** *J Phys Chem* 1995, **99**:9221–9229.
41. Schönhoff M, Chi LF, Fuchs H, Lösche M: **Structural rearrangements upon photoreorientation of amphiphilic azobenzene dyes organized in ultrathin films on solid surfaces.** *Langmuir* 1995, **11**:163–168.
42. Tabe Y, Yokoyama H: **Two-dimensional dynamic patterns in illuminated Langmuir monolayers.** *Langmuir* 1995, **11**:4609–4613.

The authors describe a static stripe texture in monolayers of an amphiphilic azobenzene derivative observed by polarized reflection microscopy. Structural changes upon prolonged illumination of the monolayer, giving rise to photoisomerization of the dye, generate sustained travelling waves associated with variations of the molecular tilt orientation.